Effect of Droplet Deformation on the Interactions in Microemulsions[1]

NIKOLAI D. DENKOV, PETER A. KRALCHEVSKY, IVAN B. IVANOV,[2] AND CHRISTIAN S. VASSILIEFF[3]

Laboratory of Thermodynamics and Physicochemical Hydrodynamics, Faculty of Chemistry, University of Sofia, Sofia 1126, Bulgaria

Received February 9, 1990; accepted August 3, 1990

The deformability of droplets is accounted for as a new effect in the statistical mechanics of microemulsions. It is assumed that a plane-parallel film is formed between two colliding microemulsion droplets. The collision is accompanied by deformation of the droplets and by an increase of their interfacial area. The increased interfacial energy gives rise to an effective soft repulsion between the two droplets. In addition, the deformed droplets, having the shape of spherical segments, exhibit considerably greater van der Waals attraction than two spheres of the same volume, separated at the same surface-to-surface distance. The superposition of these two effects leads to the appearance of a potential well in the energy of droplet–droplet interaction. The latter depends on the droplet interfacial tension, the Gibbs elasticity, the Hamaker constant, and the thickness of the liquid film separating the droplets. The soft repulsion and the increased attraction predicted by this model lead to pronouncedly lower values of the calculated second virial coefficient in comparison with the hard sphere model of microemulsions. The deformable droplet model proposed in this paper allows the explanation of experimental findings such as the abnormally low measured values of the second virial and diffusion coefficients as well as the dimer formation in microemulsions.

1. INTRODUCTION

The knowledge of the potential of interaction between particles is of crucial importance in the statistical theories of microemulsions (see, e.g., (1–3)). Among the numerous methods for investigation of these interactions, the static and dynamic light scattering techniques are probably the most versatile, for they allow measurement of the virial and diffusion coefficients and the radius of the particles (4, 5). The theoretical basis of the calculation of interaction energy from light scattering data was laid by Calje *et al.* (6). They used the model of nondeformable hard spheres interacting through van der Waals attraction (the electrostatic interaction is missing in the case of W/O microemulsions). These authors met two major difficulties in the interpretation of their experimental data: (i) The difference between the hard sphere radius, calculated by them, and the water core radius of the droplets was considerably smaller than the chain length of the surfactant molecule. (ii) To fit the experimental curve they had to use a very large value of the Hamaker constant: 1.75×10^{-19} J, which is more than 10 times higher than the value generally accepted now (see Section 5). Similar systematic deviations were observed by later investigators (4, 5, 7–9). For instance, Ober and Taupin (8) and Hou *et al.* (9) used values 1×10^{-18} and 4.6×10^{-19} J, respectively, for the Hamaker constant. Besides, Cazabat and Langevin (5, 7) and Brunetti *et al.* (4) found that the measured diffusion coefficients were always considerably smaller than those calculated from Felderhof's

[1] Part of this work was presented as an invited lecture at the Sixth International Symposium on Surfactants in Solution, New Delhi, India, 1986.

[2] Author to whom correspondence should be addressed.

[3] Present address: Department of Physical Chemistry, Faculty of Chemistry, University of Sofia, Sofia 1126, Bulgaria.

0021-9797/91 $3.00

theory (10), which is based on the hard sphere model.

Another experimental observation, which can hardly be explained in the framework of the hard sphere model, is the formation of transient dimers, which was revealed by SANS-scattering (8), self diffusion, and electric birefringence measurements (11, 12). Such dimers were found in considerable amount even in ternary systems (without cosurfactant) (11). Their presence is even more probable in quaternary systems with large attractive interactions (11), where they can lead to percolative behavior of the electric conductivity (1, 7) and even to the formation of random bicontinuous structures (13). The equilibrium constant of dimer formation (14, 15), just like the second virial coefficient (see Eq. [4.2] below), depends on the energy of interaction between the droplets. It is obvious then, that in the framework of the hard sphere model abnormally high values of the Hamaker constant will be needed to explain the dimer formation.

Another (indirect) argument in favor of the formation of dimers is the exchange of material between colliding droplets, which was evidenced by electric conductivity (16) and electric induced birefringence measurements (7, 11) and by chemical methods (17, 18). The exchange of material is believed to occur through transient pores that form between the colliding drops (17, 18). In the hard sphere model the area of contact is zero (point contact) so that the probability of pore formation will be negligible.

When it became increasingly clear that the simple hard sphere model could not explain all these findings, several more sophisticated models were proposed. To account for the strong attraction between the droplets Bothorel and co-workers (19) assumed that during collision the layers adsorbed on the two droplets interpenetrate each other, which leads to an increased value of the Hamaker constant in the region of overlapping. Much attention has been given to Helfrich's idea (20) about the spontaneous curvature and the bending energy (see e.g., (21–25)). Auvray (14) applied this idea to calculate the equilibrium constant for the formation of transient dimers by assuming that two droplets partially coalesce to form a larger drop. Another effect that has been accounted for is the thermal fluctuations of the drop surfaces (18, 26, 27).

One fact that has been disregarded so far in the theories using the droplet model is the following. Whatever the final result of the collision (rebound, partial or total coalescence), each drop colliding fronts must deform and flatten when the two drops come close to each other. This effect, which leads to the formation of an (almost) planar film between the two drops, has been extensively studied in the hydrodynamic theory of macroemulsions and foams (for a review see (28)). It is true that the width of the gap between the drops, where such a film forms, decreases strongly with the drop radius, but because of the very low interfacial tension of the microemulsions, thin films can form between colliding droplets at reasonable gap widths (for a numerical estimate see Section 7). This process should be facilitated by the high fluidity of the droplet interfaces (21, 29, 30).

The formation of such a thin film alters the configuration of the system (as compared with the hard sphere model) and hence the occurrence of the collision process, including the rate of approach of the two droplets. We will discuss briefly in Section 7 some of these effects. However, the main goal of the present paper is more modest: we want to derive an expression for the potential energy of interaction between two deformed droplets (Section 3) and to apply it to a calculation of the second virial coefficient (Section 4). It will be shown in Section 6 that with a reasonable choice of the system parameters our model not only yields numerical values of the virial coefficient B close to those measured experimentally by Bothorel and coworkers (4, 19, 31), but also predicts correctly the dependence of B on the droplet radius.

We believe that other effects, such as spontaneous curvature, bending energy, etc., are

also important and should be incorporated in the theory. Although this could be done relatively easily, we will not attempt such a generalization for two major reasons. First, because then the theory will lose its simplicity and the effect of the deformability of the droplets will become less evident for the reader. Second, because the numerical calculations will involve the use of more adjustable parameters.

For similar reasons we will not investigate the stability of the thin film between the droplets. In principle its rupture (leading to total or partial fusion of the drops) can be caused either by the formation in the film of holes (see, e.g., (32)) or by capillary waves (33–35). These processes can be treated theoretically by methods already developed for thin films (33–35) and biological membranes (32).

2. DESCRIPTION OF THE DROPLET DEFORMATION

A widely accepted scheme (4) for droplets of water in oil (W/O) microemulsions is shown in Fig. 1: a water core, covered by a mixed adsorbed layer consisting of a surfactant (the one with longer hydrocarbon chain) and a cosurfactant (usually an alcohol with a shorter chain), the whole embedded in the continuous oil phase, containing also cosurfactant. Some surfactants, such as AOT, can form microemulsions without cosurfactants (36–38). Since the radius of the water core is very small (5–10 nm) and comparable to the lengths of the surfactant and alcohol molecules, and since quite often different equations refer to different surfaces (i.e., to different radii), one must always specify which radius is being used. The radius of the outermost sphere, corresponding to the fully extended surfactant molecule, is usually close to the so-called "hydrodynamic radius," R_h, measured by dynamic light scattering (4, 5). The radius of the equimolecular dividing surface, R_0, for which the adsorption of water is zero, in the framework of this model is approximately equal to the radius of the water core. Another important radius (not shown in Fig. 1) is that of the surface of tension, R_t (see (39–41) for definition), i.e., the surface for which the interfacial bending moment is zero (42). Unfortunately, the exact location of the surface of tension is so far unknown, although approximate theories are available (23, 24).

We consider now the following process. Two microemulsion droplets in an unbounded continuous phase undergo central collision. When they come close to each other the hydrodynamic resistance leads to deformation of their colliding fronts and a planar film forms (Fig. 2). The film radius r_c increases as the two droplets come closer to each other. When the repulsion energy, generated by the increased droplet area and interfacial tension (for more details, see below), becomes equal to the initial kinetic energy, say kT (k is the Boltzmann constant and T is temperature), the motion of the droplets changes its direction. They either rebound back to an infinite distance or form an oscillating dimer if the depth of the potential well is of the order of or larger than kT.

We propose the following model for droplet deformation during the collision. First of all it is natural to assume that the liquid phases are incompressible, in particular, the volume, v_w, of the water core of each microemulsion droplet does not change during the collision. If R_0 is the radius of the water core of a spher-

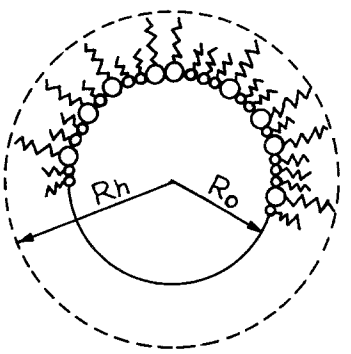

FIG. 1. Sketch of a water-in-oil microemulsion droplet. R_0 is the radius of the water core and R_h is the hydrodynamic drop radius.

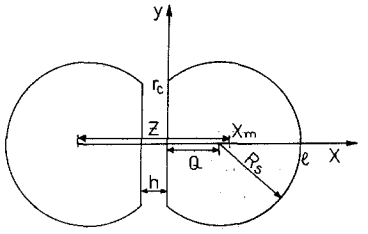

FIG. 2. Model of two deformed microemulsion droplets having the shape of spherical segments of radius R_s. z is the distance between the mass centers; r_c and h are the radius and the thickness of the film between the droplets.

ical microemulsion droplet before the collision, then

$$v_w = \frac{4}{3}\pi R_0^3 = \text{const.} \qquad [2.1]$$

Further, we assume that the droplet surface consists of two parts: (i) flat film surface, which is a circle of radius r_c, and (ii) spherical part of radius R_s, which varies during droplet deformation—see Fig. 2. R_s is the radius of the water core of the deformed droplet. Assumption (ii) means that the viscous stresses acting on the outer (spherical) parts of the droplets are negligible compared with the capillary pressure.

To describe mathematically the deformation, let us choose the coordinate system as shown in Fig. 2. The film surface corresponds to x = 0 and the outer spherical surface satisfies the equation

$$(x - Q)^2 + y^2 = (l - Q)^2, \qquad [2.2]$$

where Q is the coordinate of the center of the outer spherical surface and

$$l = Q + R_s \qquad [2.3]$$

The volume of a deformed droplet is

$$v_w = \pi \int_0^l y^2(x)dx = \pi\left(\frac{2}{3}l - Q\right)l^2, \qquad [2.4]$$

where the generatrix $y(x)$ of the outer spherical surface is determined by Eq. [2.2]. The elimination of V_w between Eqs. [2.1] and [2.4] yields

$$Q = \frac{2}{3}l - 4R_0^3/3l^2 \qquad [2.5]$$

By substitution of this expression for Q into Eq. [2.3] one obtains

$$R_s = l/3 + 4R_0^3/3l^2. \qquad [2.6]$$

In addition, by means of Eqs. [2.5] and [2.6] one derives

$$r_c = (R_s^2 - Q^2)^{1/2}$$
$$= (8R_0^3/3l - l^2/3)^{1/2}. \qquad [2.7]$$

From a mechanical viewpoint it is reasonable to characterize the distance between two interacting droplets by the distance between their centers of masses. At constant density of the liquid the coordinate, x_m, of the mass center of a droplet is defined by the expression

$$x_m = \frac{1}{v_w}\pi \int_0^l xy^2(x)dx. \qquad [2.8]$$

By substitution of y^2 from Eq. [2.2] into Eq. [2.8] and carrying out the integration one obtains

$$x_m = \frac{\pi}{v_w}\left[\frac{1}{2}(l - 2Q)l^3 + \frac{2}{3}Ql^3 - \frac{1}{4}l^4\right]. \qquad [2.9]$$

The total distance between the mass centers of two droplets of equal size is

$$z = 2x_m + h, \qquad [2.10]$$

where h is the film thickness—Fig. 2. By means of Eqs. [2.5] and [2.9] one can transform Eq. [2.10] to read

$$z = \frac{2}{3}l + l^4/24R_0^3 + h \quad \text{at } l < 2R_0. \qquad [2.11]$$

One sees that if the droplet deformation is characterized by the parameter l, the other geometrical parameters, Q, R_s, r_c, and z, can be calculated from Eqs. [2.5]–[2.7] and [2.11] as functions of l. We will use this result in Section 4 below to calculate the second virial coefficient. To do that we need an expression

for the potential energy of droplet–droplet interaction.

3. POTENTIAL ENERGY OF TWO COLLIDING DROPLETS

To calculate the energy, W, of interaction between two water-in-oil microemulsion droplets we will suppose that the system under consideration satisfies the following conditions:

(i) The surfactant is present only at the interface, where it is evenly distributed. This assumption is generally accepted in the literature (9, 21, 36); it is supported by the measurements of Biais *et al.* (48), who determined the compositions of the continuous phase, water core and surfactant layer, separately.

(ii) The interface, which is newly created during the deformation, is immediately filled with alcohol. Such an assumption is supported by the finding of Zana and Lang (17) that the alcohol adsorption is a very fast process with a characteristic time of the order of 10^{-8} to 10^{-9} s.

(iii) The thickness h of the planar film formed between two colliding droplets remains constant during the process of deformation. As discussed in Section 7 below, this assumption can be supported by the hydrodynamics of interaction between fluid particles. In particular, the constancy of h is due to the considerable viscous stresses preventing the thinning of the film.

Under these conditions the potential energy of two interacting droplets can be presented as a superposition of two terms:

$$W = W^s + W^{vw}. \qquad [3.1]$$

Here W^s is the deformation energy due to the extension of the interfacial layer and W^{vw} is the energy of van der Waals interaction between the two droplets. Expressions for W^s and W^{vw} are derived below.

(a) Work for Extension of the Interfacial Layer

W^s is the work for extension of the interfacial layer from an initial (nondeformed) state "I" with interfacial tension σ_0 to an instantaneous (deformed) state "II." Then obviously

$$W^s = \int_I^{II} \sigma dA, \qquad [3.2]$$

where A and σ are area and interfacial tension of the adsorbed layer. Calculation of the integral in Eq. [3.2] is possible only if the equation of state of the adsorbed layer is known. For the time being we will adopt the simplest possible approach, by assuming that the Gibbs elasticity

$$E_G = -d\sigma/d(\ln \Gamma_s) \qquad [3.3]$$

remains constant during the collision; here

$$\Gamma_s = N_s/A \qquad [3.4]$$

is the surfactant adsorption, with N_s being the total number of adsorbed surfactant molecules. Since N_s was assumed to be constant during the collision, an integration of Eq. [3.3] for the process of extension I → II yields

$$\sigma(A) - \sigma_0 = E_G \ln (A/A_0), \qquad [3.5]$$

where

$$A_0 = 4\pi R_0^2 \qquad [3.6]$$

is the area of a nondeformed droplet. Then substitution from [3.5] into [3.2] gives

$$W^s = (\sigma_0 - E_G)(A - A_0) + E_G A \ln(A/A_0). \qquad [3.7]$$

At relatively small extensions, i.e., at $\Delta A/A_0 \ll 1$, where

$$\Delta A = A - A_0. \qquad [3.8]$$

Eq. [3.7] yields

$$W^s = \sigma_0 \Delta A + \frac{1}{2} E_G A_0 (\Delta A/A_0)^2 + \ldots. \qquad [3.9]$$

The first term on the right-hand side of Eq. [3.9] accounts for the contribution of the increased surface area, whereas the second one accounts for the contribution of the Gibbs elasticity.

To calculate W^s as a function of the parameter l one must use the expression

$$A = \pi r_c^2 + 2\pi R_s(R_s + Q) \quad [3.10]$$

(see Fig. 2) along with Eqs. [2.5]–[2.7].

(b) Van der Waals Interaction between Two Deformed Drops

According to Hamaker (43, 44) the total energy of van der Waals interaction between two bodies immersed in a fluid medium can be calculated by means of the integral expression

$$W^{vw} = -(1/\pi^2)\int_{V_1}\int_{V_2}\frac{A_H d\mathbf{r}_1 d\mathbf{r}_2}{|\mathbf{r}_1 - \mathbf{r}_2|^6}, \quad [3.11]$$

where A_H is the Hamaker constant, $\mathbf{r}_1(\mathbf{r}_2)$ is the position vector of a point from the first (second) body, and the integration is carried out over the volumes V_1 and V_2 of the two bodies. For two homogeneous spheres of the same radius R_0, Eq. [3.11] yields the known Hamaker formula (43)

$$W_H^{vw} = -A_H G_0(s), \quad [3.12]$$

where

$$G_0(s) = \frac{1}{12}\{1/(s^2 + 2s) + 1/(s^2 + 2s + 1) + 2\ln[1 - 1/(s^2 + 2s + 1)]\}, \quad [3.13]$$

$$s = h/2R_0, \quad [3.14]$$

with h being the gap width between the fore points of the two droplets.

For two deformed spheres, like those shown in Fig. 2, we expanded the integral in Eq. [3.11] for $(r_c/R_0) \ll 1$ and derived (see the Appendix) the expression for the van der Waals interaction energy

$$W^{vw} = -A_H[G_0(s) + G_1(s)(r_c/R_0)^2 + O(r_c^4/R_0^4)], \quad [3.15]$$

where $G_1(s)$ is a universal function of s defined as

$$G_1(s) = \int_0^1 d\rho_1 \int_0^1 d\rho_2 \times \int_{q_1(\rho_2)}^{q_2(\rho_1)} d\zeta_1 [F(\rho_1, \rho_2, \zeta_1, -q_1(\rho_2)) - F(\rho_1, \rho_2, \zeta_1, -q_2(\rho_2))], \quad [3.16]$$

where

$$q_1 = 1 + s - \sqrt{1 - \rho^2},$$
$$q_2(\rho) = 1 + s + \sqrt{1 - \rho^2} \quad [3.17]$$

$$F(\rho_1, \rho_2, \zeta_1, \zeta_2) = 4\rho_1\rho_2/[L(\rho_1, \rho_2, \zeta_1, \zeta_2)]^3 + 24\rho_1^3\rho_2^3/[L(\rho_1, \rho_2, \zeta_1, \zeta_2)]^5 \quad [3.18]$$

$$L(\rho_1, \rho_2, \zeta_1, \zeta_2) = \{[(\rho_1 + \rho_2)^2 + (\zeta_1 - \zeta_2)^2] \times [(\rho_1 - \rho_2)^2 + (\zeta_1 - \zeta_2)^2]\}^{1/2}. \quad [3.19]$$

We calculated $G_1(s)$ from Eqs. [3.16]–[3.19] by using numerical integration. The plot of $G_1(s)/G_0(s)$ is shown in Fig. 3.

To check the accuracy of Eq. [3.15], where the terms of the order of r_c^4/R_0^4 (and of higher orders) are neglected, we compared the values of W^{vw}, calculated by means of the approximated Eq. [3.15], with the exact values, calculated by computer integration of Eq.

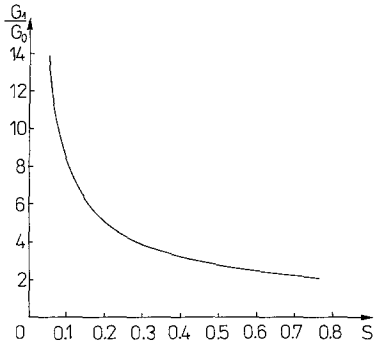

FIG. 3. Plot of G_1/G_0 vs. s calculated by numerical integration of Eq. [3.16] along with Eqs. [3.13] and [3.17]–[3.19].

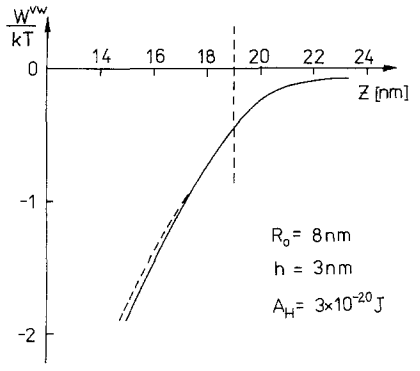

FIG. 4. Examination of the accuracy of the approximated Eq. [3.15] (the dashed line) against the exact curve calculated by numerical integration of Eq. [3.11] (the solid line). $z < 19$ nm corresponds to deformed drops.

[3.11]—see Fig. 4. The result shows that the approximated Eq. [3.15] holds with a very good accuracy for a set of typical values of the parameters characterizing the two interacting droplets ($R_0 = 8$ nm, $h = 3$ nm, $A_H = 3 \times 10^{-20}$ J). This fact makes Eq. [3.15] appropriate for our calculations below.

(c) Procedure for Calculation of $W(z)$

To calculate the interaction energy W, we must express it as a function of the distance z between the centers of mass of the two drops. This can be done by the following procedure.

(i) Before the deformation, z is the distance between the centers of the two spherical drops. W^s is zero in this case. Then in accordance with Eq. [3.1] $W = W^{vw}$, W^{vw} must be calculated by means of the Hamaker formula [3.12] along with Eqs. [3.13] and [3.14].

(ii) When the particles are deformed z is determined by Eq. [2.11] for each value of l. The geometrical parameters Q, R_s, r_c and A can be calculated by means of Eqs. [2.5]–[2.7] and [3.10] for the same value of l. Then Eq. [3.7] yields $W^s = W^s(z)$ and Eqs. [3.14]–[3.15] yield $W^{vw} = W^{vw}(z)$ for a given value of h. Finally one calculates $W(z)$ by using Eq. [3.1].

4. THE SECOND VIRIAL COEFFICIENT

The usual virial expansion (15)

$$\Pi/kT = \rho + \frac{1}{2}\beta\rho^2 + \cdots \qquad [4.1]$$

can be applied to characterize the dependence of the osmotic pressure Π on the number density ρ of the microemulsion droplets. The statistical mechanics provides the following expression for the second virial coefficient β:

$$\beta = \int_0^\infty [1 - \exp(-W/kT)]4\pi z^2 dz \qquad [4.2]$$

One can determine the second virial coefficient β by carrying out the integration in Eq. [4.2] numerically. The values of β calculated in this way are to be compared with those determined by light scattering. However, β is not directly determined from the experimental data. This problem is discussed below.

The basic equation used for interpreting the light scattering data is (45)

$$R_{90°} = 2\pi^2 n^2 \left(\frac{\partial n}{\partial \rho}\right)^2 \rho \Big/ \left[\lambda_0^4 \frac{1}{kT}\left(\frac{\partial \Pi}{\partial \rho}\right)\right] \qquad [4.3]$$

Here $R_{90°}$ is the Rayleigh ratio, corresponding to light scattering at 90°; n is the refractive index of the solution (the microemulsion); λ_0 is the light wavelength in vacuum. By using Eq. [4.1] one can transform Eq. [4.3] to read

$$\rho K_\rho / R_{90°} = 1 + \beta\rho + \ldots, \qquad [4.4]$$

where

$$K_\rho = 2\pi^2 n^2 \left(\frac{\partial n}{\partial \rho}\right)^2 \Big/ \lambda_0^4. \qquad [4.5]$$

In principle one can determine β from the slope of the plot of $\rho K_\rho / R_{90°}$ vs. ρ—see Eq. [4.4]. However, the number density is not directly given by the experiment. A much more convenient measure for the concentration of the water-in-oil microemulsion droplets is the volume fraction of the water,

$$\phi_w = v_w \rho \qquad [4.6]$$

where v_w is the volume of the water core of a

microemulsion droplet. If $\rho = \phi_w/v_w$ is substituted in Eq. [4.4], one can derive

$$\phi_w K_w/R_{90^\circ} = \frac{1}{v_w}(1 + B_w\phi_w) \quad [4.7]$$

with

$$B_w = \beta/v_w \quad [4.8]$$

and

$$K_w = 2\pi^2 n^2\left(\frac{\partial n}{\partial \phi_w}\right)^2 \Big/ \lambda_0^4. \quad [4.9]$$

Both ϕ_w and $(\phi_w K_w)/R_{90^\circ}$ are liable to direct measurement, and then one can determine B_w by processing the data according to Eq. [4.7]. In Section 6 below we will compare the experimental values of B_w with the ones calculated from Eqs. [4.2] and [4.8] by using our model expression for the interaction energy $W(z)$.

It is worth noting that some authors (4, 5, 7, 19, 31) prefer to use another measure,

$$\phi_d = v_d\rho, \quad [4.10]$$

for the concentration of the microemulsion droplets. In contrast to v_w (cf. Eq. [4.6]) v_d includes not only the volume of the water core, but also the volume of the surfactant and cosurfactant adsorbed at the surface of the microemulsion droplet. That is why in some cases one can have $v_d \approx 2v_w$; i.e., the difference between v_d and v_w can be considerable. By means of Eq. [4.10] one can transform Eq. [4.4] to read

$$\phi_d K_d/R_{90^\circ} = \frac{1}{v_d}(1 + B_d\phi_d) \quad [4.11]$$

with

$$B_d = \beta/v_d \quad [4.12]$$

and

$$K_d = 2\pi^2 n^2\left(\frac{\partial n}{\partial \phi_d}\right)^2 \Big/ \lambda_0^4. \quad [4.13]$$

The light scattering data in Refs. (4, 5, 7, 19, 31) were processed in accordance with Eq. [4.11] and the values of v_d and B_d were determined. Therefore when we compared our model with the data from Refs. (4, 19, 31), we calculated B_w from the data for B_d by using the equation

$$B_w = \frac{v_d}{v_w}B_d = \frac{\phi_d}{\phi_w}B_d. \quad [4.14]$$

Eq. [4.14] is a corollary from Eqs. [4.6], [4.8], [4.10], and [4.12]. Eq. [4.14] shows that B_w is always larger than B_d. In spite of the fact that each of the quantities β, B_w, and B_d is called "second virial coefficient," one must consider the differences in their definitions when comparing theory with experiment.

Obviously

$$R_0/R_d = (v_w/v_d)^{1/3} = (\phi_w/\phi_d)^{1/3}. \quad [4.15]$$

We used Eq. [4.15] to calculate R_0 from the data for R_d given in Refs. (4, 19, 31).

5. CHOICE OF THE SYSTEM PARAMETERS

Systematic studies of the dependence of the virial coefficient on the cosurfactant chain length, the drop size, and the system composition were carried out by Bothorel and coworkers (4, 19, 31). They studied W/O microemulsions with surfactant sodium dodecylsulfate (SDS) and various normal middle chain alcohols as cosurfactants: pentanol, hexanol, and heptanol. We will attempt to compare the predictions of our model with their results. This determines our choice of the system parameters. In the experiments of Bothorel and coworkers the radius of the water core R_0 varies from 3.5 to 7 nm. There are no data for the interfacial tension σ_0 of the microemulsion drop but it is widely accepted (21, 23, 24) that it is lower than 0.1 mN/m. Our calculations showed that below 0.05 mN/m the value of σ_0 has no effect on the calculated virial coefficients. We will use the value $\sigma_0 = 0.01$ mN/m.

The values of the Hamaker constant A_H for the system water/oil/water are of the order of 10^{-20} J (8, 44, 46). We will vary A_H in the range 2×10^{-20} J to 5×10^{-20} J. As to the thickness h of the hydrocarbon film between the water cores, it will be 3 nm if the extended

chains of the surfactant (SDS) on the two droplet surfaces touch each other, and 2 nm if there is interpenetration of the two adsorbed layers; in the former case it equals twice the chain length of the surfactant molecule and in the latter case it equals the sum of the chain lengths of the surfactant and cosurfactant molecules. However, since according to our model the surfactant polar heads are also included in the film (see Section 2), the film thickness h will be somewhat higher. Thus we varied h between 2.2 and 3.4 nm.

To determine B_w from Eq. [4.14] and R_0 from Eq. [4.15] we need the value of the ratio ϕ_d/ϕ_w. It is easy to calculate this ratio using the data for the composition of the microemulsion droplets measured in Refs. (4, 19, 31) by the so-called "dilution procedure" (47).

The most difficult and probably the most important problems are connected with the Gibbs elasticity E_G. According to our assumptions in Section 3, the number of surfactant molecules N_s at the interface remains constant during the collision. Apparently, under these conditions the interfacial tensions σ and σ_0 in Eq. [3.5] should depend only on the surfactant adsorption Γ_s, the adsorbed alcohol playing the role of a "surface" solvent. Indeed, Saraga (49) found for the interfacial tension of the interface water/dodecane with surfactant sodium docosylsulfate and cosurfactant pentanol the equation of state

$$\sigma_p - \sigma = 3kT\Gamma_s, \qquad [5.1]$$

where σ_p is the interfacial tension water/dodecane. By applying Eq. [5.1] to a deformed drop with interfacial tension σ one obtains (cf. Eqs. [3.5] and [3.8])

$$\sigma - \sigma_0 = E_G(\Delta A/A), \qquad [5.2]$$

where

$$E_G = 3kT(N_s/A) \qquad [5.3]$$

is the Gibbs elasticity of the nondeformed drop. If $\Gamma_s^{-1} = 0.64$ nm^2 (31, 50), Eq. [5.3] yields $E_G = 20$ mN/m. However, Eq. [5.1] turned out to be applicable only up to pentanol concentrations 0.025 M. At higher alcohol concentrations E_G drops to 15 mN/m. On the other hand, from Eq. (5.11) of Davies and Rideal (51), which refers to adsorbed layers of SDS at the water/dodecane interface, with $\Gamma_s^{-1} = 0.64$ nm^2 one finds $E_G = 39$ mN/m. Finally, E_G can depend also on the chain length of the alcohol. That is why we varied E_G between 10 and 40 mN/m. When varying the other parameters, we used $E_G = 20$ mN/m, because the system studied by Saraga is the closest to that studied by Bothorel and coworkers.

6. NUMERICAL RESULTS

The result for the interaction energy W vs. the distance z between the centers of mass of the liquid cores of two deformed droplets is illustrated in Fig. 5. The procedure outlined in Section 3c was applied to calculate $W(z)$. Typical values of the system parameters for a water-in-oil microemulsion are used. The initial radius of the nondeformed droplet is $R_0 = 8$ nm. In accordance with the discussion in the previous section we used $h = 3$ nm, $A_H = 3 \times 10^{-20}$ J, $E_G = 20$ mN/m, $\sigma_0 = 0.01$ mN/m. In particular, by using Eq. [3.14] one calculates $s = 0.1875$ and then from Fig. 3 one finds $G_1(s)/G_0(s) = 5.25$. The latter value was used in Eq. [3.15] for the calculation of

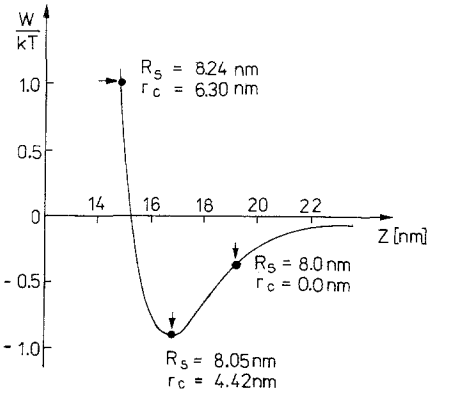

FIG. 5. The potential energy of interaction of two colliding deformable microemulsion droplets, W, vs. the distance z between the mass centers of the droplets (k is the Boltzmann constant, $T = 25$°C).

$W^{vw}(z)$ at each given value of $r_c = r_c(z)$. As shown in Fig. 5 the deformation starts at $z = 19$ nm ($r_c = 0$). At $z = 16.8$ nm $W(z)$ has a minimum value of $-0.9\ kT$, which is due to the compensation between the attractive van der Waals energy W^{vw} and the effective repulsive energy W^s due to the extension of the droplet interfaces—cf. Eq. [3.1]. For $z < 15.2$ nm the repulsive energy prevails and $W(z)$ is positive. The values of R_s and r_c calculated from Eqs. [2.6] and [2.7] are shown in Fig. 5 for three points denoted by arrows.

The most remarkable feature of the curve $W(z)$ is the presence of a potential minimum whose depth is of the order of kT. Note that the absolute minimum value of $W(z)$, corresponding to the hard sphere model, is equal to $0.3\ kT$. That is considerably smaller than the value on our curve $W(z)$. The occurrence of such a deep minimum means that the formation of relatively stable dimers is quite probable. The film separating the droplets could rupture and the drops could merge to a single larger drop, but as we specified in the Introduction we will not consider this process.

The point with $R_s = 8.24$ nm and $r_c = 6.30$ nm shown in Fig. 5 corresponds to $W(z) = kT$. This point can be approximately interpreted as the point of recoil of two colliding particles. The calculated difference $R_s - R_0 = 0.24$ nm at this point is only 3% of the value of R_0. Hence, the effective repulsive force at the moment of recoil is a result of a not too large extension of the drop surface.

From the interaction energy $W(z)$ we calculated the virial coefficient $B_w = \beta/v_w$ by using Eq. [4.2]. We have studied the effects of three parameters: Hamaker constant A_H, film thickness h, and Gibbs elasticity E_G. In Figs. 6 to 8 our results are compared with the experimental data of Bothorel *et al.* (4, 19) for the system water/dodecane/sodium dodecylsulfate and two different cosurfactants: hexanol (open circles) and heptanol (full circles). Experimentally determined points are recalculated according to the discussion in Section 4. Similar data with the same trend of the dependence of B vs. R were reported by Cazabat and Langevin (5, 7) and Hou *et al.* (9) for other systems.

Fig. 6 represents the calculated curves B_w vs. R_0 for four different values of A_H between 2 and 5×10^{-20} J. The values of the other parameters are fixed as follows: $h = 3$ nm, $\sigma_0 = 0.01$ mN/m, and $E_G = 20$ mN/m. One sees that the theoretical curves follow the trend of the experimental data for B_w vs. R_0. Besides, the larger the Hamaker constant A_H the smaller B_w, as should be expected.

The role of the Gibbs elasticity, E_G, is illustrated in Fig. 7 for four different values of E_G at fixed $h = 3$ nm, $\sigma_0 = 0.01$ mN/m, $A_H = 3 \times 10^{-20}$ J. According to our model the interfacial Gibbs elasticity is a source of an effective soft repulsion between the droplets. The theoretical curves show that the larger the Gibbs elasticity, the greater the second virial coefficient B_w.

The strong effect of the film thickness h on B_w is illustrated in Fig. 8, where the four solid lines represent B_w vs. R_0 for deformable droplets, whereas the two dashed lines are calculated for two nondeformed spherical droplets by using Eqs. [3.12]–[3.14], with h being the shortest distance between them. The values of B_w for the nondeformed droplets (corresponding to the hard sphere model) are pronouncedly larger than those for the deformed

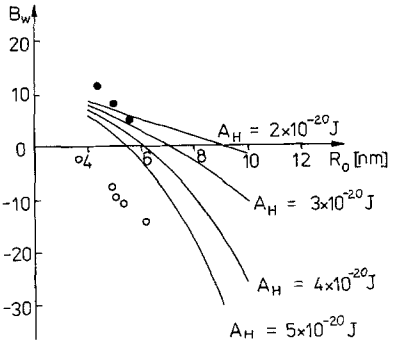

FIG. 6. Dimensionless second virial coefficient B_w vs. drop radius R_0 calculated at different values of the Hamaker constant A_H. The full and open circles are experimental data from (4, 19, 31) with cosurfactant heptanol and hexanol, respectively.

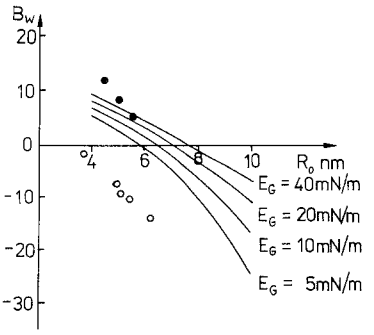

FIG. 7. Dimensionless second virial coefficient B_w vs. drop radius R_0 calculated at different values of the Gibbs elasticity E_G. The full and open circles are experimental data from (4, 19, 31) with cosurfactant heptanol and hexanol, respectively.

droplets. The values of the fixed parameters are $A_H = 3 \times 10^{-20}$ J, $\sigma_0 = 0.01$ mN/m, $E_G = 20$ mN/m. One sees in Fig. 8 that the smaller h the less B_w.

The numerical data presented in Figs. 6 to 8 show that the deformation of the drops during collision and the ensuing effects on W and B_w can be at least as important as the other effects considered by previous authors. In general we could have fitted the experimental data of Bothorel *et al.* (4, 19) by varying the parameters A_H, h, and E_G in a relatively narrow, physically reasonable range. As already pointed out in Section 1 we did not attempt that, because we are fully aware of the crudeness of our calculations, especially in determining W^s. Besides, we think that other effects, such as spontaneous curvature, bending energy of the drop surface, and thermal fluctuations (20, 21, 23, 26, 27), must be properly incorporated in the model of the deformable droplets in order to reach a more realistic description of the droplet–droplet interactions in microemulsions. Such studies are now under way.

7. DISCUSSION

We believe that the major merit of our model is that it explains (at least qualitatively in its present form) in a natural way many of the experimental observations. First of all, it reveals the origin of the repulsion between the droplets. It is hard to believe that drops with interfacial tension as low as 0.1–0.01 mN/m could collide like hard spheres. We have shown in Section 3 that the repulsion is due to the deformation and stems both from the increased droplet area and from the Gibbs elasticity of the adsorbed layers—see Eq. [3.9].

Besides, we do not need to refer to the concept of interpenetration of the adsorbed layers either to explain the measured values of the virial coefficient or to interpret the observed differences between the hydrodynamic radius of the droplet and the hard sphere radius determined by light scattering experiments (4, 6, 7, 19). In spite of being possible such an interpenetration is probably very small. Indeed, for a planar film the osmotic Gibbs free energy, ΔG_{osm}, due to interpenetration of the surfactant hydrocarbon chains is (52, 53)

$$\frac{\Delta G_{osm}}{kT} = \frac{2\varphi_c^2}{v_s}\left(\frac{1}{2} - \chi\right)A^f \Delta h,$$

where φ_c is the volume fraction of chains in the outmost part of the surfactant layer (see Fig. 1), v_s is the volume of a solvent molecule, χ is the mixing parameter, $A^f = \pi r_c^2$ is the film area, and Δh is the decrease of film thickness due to the interpenetration. If $\chi = 0$ (ideal solution), the interpenetration stops when

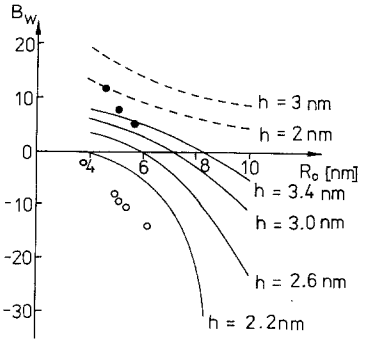

FIG. 8. Dimensionless second virial coefficient B_w vs. drop radius R_0 calculated at different values of the film thickness h. The full and open circles are experimental data from (4, 19, 31) with cosurfactant heptanol and hexanol, respectively. The dashed lines correspond to nondeformed spheres.

$\Delta G_{osm}/kT = 1$, i.e., when $\Delta h = v_s/\varphi_c^2 A^f$. For $r_c = 3$ nm, $\varphi_c = \frac{1}{3}$ (4, 31, 50), and $v_s = 0.3$ nm^3 this yields a negligible overlapping, $\Delta h = 0.1$ nm.

We have already pointed out that our calculations of the interaction energy $W(z)$ (Fig. 5) suggest the formation of a considerable fraction of dimers. In this respect our results are in agreement with the findings of several research groups, who detected such dimers experimentally (8, 11, 12, 54). Auvray (14) tried to explain the presence of such dimers, as well as the anomalous low values of the virial coefficients, by using a totally different model: he assumed that (i) the colliding drops partially coalesce to form a dimer, (ii) the total water volume and the area of the adsorbed layer (considered as being incompressible) remain constant, and (iii) the whole process is governed only by the curvature energy. The experimental data are not sufficient to discriminate between Auvray's and our model. The two models are similar from a purely geometrical viewpoint: the surface of Auvray's elongated prolate dimer can be looked at as an envelope of a dimer consisting of two drops separated by a planar film.

Another argument in favor of dimer formation is the observed exchange of material between the colliding droplets. To explain this Eicke *et al.* (18) suggested that a transient pore appears at the contact point between the two droplets. Such an explanation is in agreement with our model, because the formation of transient pores in a planar film is much more probable than between spherical droplets.

Several studies (4, 19, 31) have shown that the longer the cosurfactant chain length the more positive the virial coefficient (see, e.g., Fig. 7, where experimental data with heptanol and hexanol are presented). The same result naturally follows from our theory, if the Gibbs elasticity for alcohols with longer chains is higher. Unfortunately we could not find data to prove this hypothesis, which otherwise seems reasonable. An indirect support of this viewpoint is the data of Shah and co-workers (29, 30) who found that the interfacial fluidity is larger with 1-pentanol than with 1-hexanol. It is worth pointing out that such an effect is compatible only with the model of deformable drops.

One question that could be raised is whether a planar film could form between such small droplets and to what extent the assumption of constant film thickness during the expansion of the contact line is a reasonable one. A definitive answer can be given only by solving the hydrodynamic problem for collision of deformable drops performing Brownian motion. It is hardly worthwhile doing that without having reliable experimental information on the details of the collision process. Some insight can be gained however from the hydrodynamic theory developed for collision of *macroscopic* bubbles and drops (28). According to this theory the fronts of the colliding drops will change the sign of their curvature and the film will start forming when the gap width between the drops becomes equal to

$$h_i = \mathbf{F}_d/2\pi\sigma_0, \qquad [7.1]$$

where $\mathbf{F}_d$ is the driving force pushing the two drops toward each other along their line of centers. The perimeter of the film expands very rapidly to reach the radius

$$r_i^2 = \mathbf{F}_d R_h/2\pi\sigma_0, \qquad [7.2]$$

where R_h is the hydrodynamic radius of the drop. This is the initial radius from which the interaction energy W should be calculated. Note, however, that r_i, corresponding to the outer ends of the surfactant molecules, is consequently larger than the contact radius r_c at this moment, since the later corresponds to the water core.

The driving force $\mathbf{F}_d$, which for microemulsions is the Brownian force, is a stochastic quantity. A rough estimate of its mean value could be obtained from our numerical calculations (see Fig. 5) which show that the initial kinetic energy kT drops to zero at distances of the order of $R_h/2$. Hence, we assume

$$\mathbf{F}_d \sim 2kT/R_h. \qquad [7.3]$$

Then

$$h_i \sim \frac{kT}{\pi\sigma_0 R_h}; \quad r_i \sim (kT/\pi\sigma_0)^{1/2}. \quad [7.4]$$

For $\sigma_0 = 0.1$ mN/m and $R_h = 9$ nm (this corresponds to water core radius $R = 7.5$ nm plus the surfactant chain length) Eq. [7.4] yields $h_i \approx 1.4$ nm and $r_i \approx 3.5$ nm, which are reasonable figures.

The next question is what will happen to the liquid film as the collision process evolves. According to Rulyov and Dukhin (55) the liquid will not be squeezed out and the film will keep its thickness constant if

$$\pi\sigma_0 h_i^2 \ll mv_i^2/2, \quad [7.5]$$

where v_i is the impact velocity. Substituting kT in the right-hand side of Eq. [7.5] and expressing h_i from Eq. [7.4] one finds that the film thickness will remain constant if

$$\frac{kT}{\pi\sigma_0 R_h} \sim \frac{h_i}{R_h} \ll 1. \quad [7.6]$$

Although this condition seems to be always fulfilled, it is worth estimating the drainage time τ_d, i.e., the time necessary for the liquid between the two drops to be squeezed out, so that the outer ends of the surfactant molecules "touch" each other. This can be done by using the Reynolds equation for the rate of thinning V_{Re} (see e.g. (28)),

$$-\frac{dh}{d\tau} = V_{Re} \sim \frac{2h_i^3 F_d}{3\pi\eta r_i^4}, \quad [7.7]$$

where τ is time. It yields (cf. also Eqs. [7.3] and [7.4])

$$\tau_d \sim \frac{h_i}{V_{Re}} \sim \frac{3\pi\eta R_h^3}{4kT}. \quad [7.8]$$

For $R_h = 9$ nm, the drainage time is 5.5×10^{-7} s. In the absence of information about the collision time, it is hard to say whether or not the liquid film intervening between the colliding drops will be squeezed out. Moreover, Eq. [7.8] refers to films with tangentially immobile surfaces, whereas the high interfacial fluidity found by Shah *et al.* (29, 30) can dramatically shorten the drainage time (for more details see (28, 35)).

Another experimental fact, that could be more easily explained by the drop deformation, is the anomalously low value of the diffusion coefficient D measured by dynamic light scattering. The dependence of D on the volume fraction ϕ is usually described by the equation (7, 10, 19)

$$D = D_0(1 + \alpha\phi), \quad [7.9]$$

where $D_0 = kT/6\pi\eta R_h$ is the Stokes–Einstein diffusion coefficient, with η being the dynamic viscosity. A theory of the diffusion virial coefficient α, based on the model of hard spheres, was published by Felderhof (10). However, Cazabat and Langevin (5, 7) found that the theoretical values were always higher than the experimental ones. In the framework of our model this discrepancy could be ascribed to the enhanced hydrodynamic resistance (compared to that in the model of hard spheres) due either to the thinning of the plane-parallel film forming before the two drops come into close contact or to the viscous friction accompanying the expansion of the contact line between the interacting droplets. Both processes have been treated theoretically for macroscopic drops (see e.g. (28)).

Eq. [7.7] determines the friction coefficient F_d/V_{Re} for two approaching deformed drops in the case when the liquid film is squeezed out. It can be used to calculate the diffusion coefficient, which we will denote by D_{Re}. Taking also into account Eq. [7.4] one thus obtains

$$\frac{D_{Re}}{D_0} = \frac{4h_i R_h}{(r_i^2/h_i)^2} = \frac{4h_i}{R_h}$$

With the numerical values used above ($R_h = 9$ nm, $h_i = 1.4$ nm) this yields $D_{Re}/D_0 \approx 0.6$. The experimental values of D_{Re}/D_0 for the system water/dodecane/sodium dodecylsulfate/hexanol measured by Bothorel *et al.* (4, 19, 31) are between 0.9 and 0.5 for volume fractions between 1% and 5%. In the above estimate of the diffusion coefficient we accounted in fact only for the hydrodynamic resistance, which in our model is the counterpart

of Oseen contribution in Felderhof's theory (10). It is not difficult to incorporate also the other Felderhof's contributions, such as the van der Waals attraction between the droplets (12). However the real situation could be much more complicated. Indeed, in the presence of a deep potential well the assembly of two interacting drops must be considered as a Brownian oscillator. This will require a totally different approach for the calculation of the diffusion coefficient.

8. CONCLUDING REMARKS

We have accounted for a new effect in the statistical mechanical theory of microemulsions—the deformability of the droplets. By assuming that the surfactant is located only at the drop surfaces and that the adsorbed cosurfactant is in diffusive equilibrium with the bulk phases we derived an expression for the potential energy of interaction, W, between two deformed droplets—see Section 3c.

According to our model a plane parallel liquid film is formed between the two colliding microemulsion droplets. During this process each of the two initially spherical droplets has the shape of a spherical segment—see Fig. 2. This deviation from the spherical shape (at constant drop volume) leads to an increase of the droplet surface and to extension of the interfacial surfactant layer. The increased interfacial energy of two deformed colliding droplets gives rise to an effective repulsive potential energy, W^s—see Eq. [3.7]. W^s depends both on the interfacial tension, σ_0, and on the Gibbs elasticity E_G.

Contribution to the total potential energy W gives also the energy of van der Waals attraction, W^{vw}, between the two droplets. To calculate W^{vw} before the collision we used the Hamaker expression, Eq. [3.12], for two spheres. The values of W^{vw} for two deformed droplets were calculated by means of Eq. [3.15], derived in the present paper. The latter equation, expressing the van der Waals interaction energy of two spherical segments, can be of independent interest for other similar problems.

The total potential energy W, calculated as explained in Section 3c, exhibits a very pronounced minimum of depth about kT–see Fig. 5. The knowledge of W enabled us to calculate the second virial coefficient. The latter is considerably smaller (more negative) than in the case of the hard sphere model of droplet–droplet interaction and depends on the Hamaker constant, A_H, Gibbs elasticity, E_G, and the film thickness, h. It turns out that the different possible definitions of the second virial coefficient (cf. Eqs. [4.8] and [4.12]) can strongly affect its value and the comparison between the theory and experiment. With reasonable choice of the system parameters (Hamaker constant, film thickness, and Gibbs elasticity) we obtained satisfactory agreement with the dependence of the virial coefficient on the drop radius found experimentally by Bothorel and co-workers (4, 19, 31) with four-component microemulsions. The model in its present form can be also applied to three-component microemulsions.

Our model allows qualitative explanations of other experimental facts. We found a rather deep potential well, which can be the reason for the dimer formation, evidenced by several authors (8, 11, 12). The low value of the diffusion coefficients (compared with those calculated from the Stokes–Einstein equation) measured by Cazabat and Langevin (5, 7) and Brunetti *et al.* (4) could be caused by the enhanced hydrodynamic resistance, due to the outflow of liquid in the narrow gap between the drops. Our model is also able to explain the increase of the virial coefficient with increasing cosurfactant chain length, provided that the Gibbs elasticity also increases, which seems to be the case.

We did not consider the role of other possible effects, such as spontaneous curvature, bending energy, etc., but they can be easily incorporated in our model.

APPENDIX: VAN DER WAALS INTERACTION BETWEEN TWO SPHERICAL SEGMENTS

Hamaker (43) applied Eq. [3.11] to derive an explicit expression, Eq. [3.12], for the en-

ergy of van der Waals interaction between two spheres. Our purpose here is to derive a similar expression for the case, when the two particles are spherical segments oriented as shown in Fig. 9.

Let us introduce cylindrical coordinates (r, θ, z) as shown in Fig. 9. In addition, if r_1, θ_1, and z_1 are the coordinates of a point from the upper particle and if r_2, θ_2, and z_2 are the coordinates of another point from the lower particle, then

$$|\mathbf{r}_1 - \mathbf{r}_2|^2 = r_1^2 + r_2^2 - 2r_1r_2\cos(\theta_2 - \theta_1) + (z_1 - z_2)^2. \quad [A.1]$$

It is convenient to introduce dimensionless variables

$$\rho_i = r_i/R_0, \quad \zeta_i = z_i/R_0, \quad i = 1, 2; \quad [A.2]$$

$$\zeta = R_s/R_0, \quad \epsilon = r_c/R_0 \quad [A.3]$$

where R_0 is the radius of the droplet before deformation. Then Eq. [A.1] can be transformed to read

$$|\mathbf{r}_1 - \mathbf{r}_2|^2 = R_0^2[\rho_1^2 + \rho_2^2 - 2\rho_1\rho_2\cos(\theta_2 - \theta_1) + (\zeta_1 - \zeta_2)^2]. \quad [A.4]$$

Eq. [3.11] shows that in general $W^{vw} = W^{vw}(s, \epsilon)$, where s is defined by Eq. [3.14]. We will seek W^{vw} in the form of an expansion with respect to the powers of ϵ, like Eq. [3.15]. We will neglect all terms of order higher than ϵ^3.

By using Eqs. [2.7] and [A.3] one can derive

$$l/R_0 = 2 - \frac{1}{2}\epsilon^2 + O(\epsilon^4). \quad [A.5]$$

A substitution of Eq. [A.5] into Eq. [2.6], along with Eq. [A.3], yields

$$\zeta = 1 + O(\epsilon^4). \quad [A.6]$$

That is why in the framework of the accepted accuracy we will set $\zeta = 1$ everywhere below.

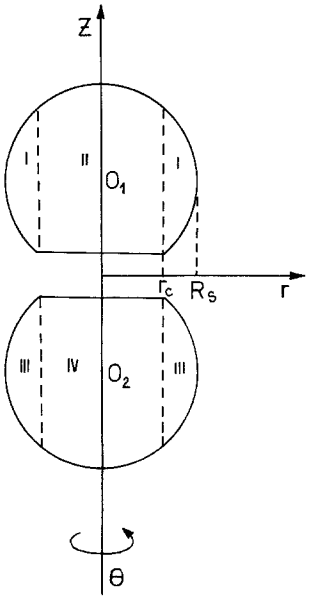

FIG. 9. Calculation of the energy of van der Waals attraction between two spherical segments (see the text).

For the geometry that we consider Eq. [3.11] can be written in the form

$$W^{vw} = -A_H[I_1(\epsilon, s) + 2I_2(\epsilon, s) + I_3(\epsilon, s)], \quad [A.7]$$

where

$$I_1(\epsilon, s) = \int_0^{\epsilon} d\rho_1 \int_0^{\epsilon} d\rho_2 \int_s^{f_2(\rho_1)} d\zeta_1 \times \int_{-f_2(\rho_2)}^{-s} d\zeta_2 F(\rho_1, \rho_2, \zeta_1, \zeta_2) \quad [A.8]$$

$$I_2(\epsilon, s) = \int_0^{\epsilon} d\rho_1 \int_{\epsilon}^{1} d\rho_2 \int_s^{f_2(\rho_1)} d\zeta_1 \times \int_{-f_2(\rho_2)}^{-f_1(\rho_2)} d\zeta_2 F(\rho_1, \rho_2, \zeta_1, \zeta_2) \quad [A.9]$$

$$I_3(\epsilon, s) = \int_{\epsilon}^{1} d\rho_1 \int_{\epsilon}^{1} d\rho_2 \int_{f_1(\rho_1)}^{f_2(\rho_1)} d\zeta_1 \times \int_{-f_2(\rho_2)}^{-f_1(\rho_2)} d\zeta_2 F(\rho_1, \rho_2, \zeta_1, \zeta_2) \quad [A.10]$$

$$f_1(\rho) = s + \sqrt{1 - \epsilon^2} - \sqrt{1 - \rho^2} \quad [A.11]$$

$$f_2(\rho) = s + \sqrt{1 - \epsilon^2} + \sqrt{1 - \rho^2} \quad [A.12]$$

and

$$F(\rho_1, \rho_2, \zeta_1, \zeta_2) = \frac{\rho_1\rho_2}{\pi^2}\int_0^{2\pi}\int_0^{2\pi} d\theta_1 d\theta_2 \times (R_0/|\mathbf{r}_1 - \mathbf{r}_2|)^6. \quad [A.13]$$

To illustrate the domains of integration in I_1, I_2, and I_3 we have divided the volumes of the two particles into regions I, II, III, and IV–see Fig. 9. Then $I_1(\epsilon, s)$ accounts for the interaction between domains II and IV, $I_2(\epsilon, s)$ for the interaction between domains II and III (or I and IV), and $I_3(\epsilon, s)$ for the interaction between domains I and III. By substitution from Eq. [A.4] into Eq. [A.13] and by carrying out the double integration one arrives at the expression [3.18] for $F(\rho_1, \rho_2, \zeta_1, \zeta_2)$.

In view of Eqs. [A.8]–[A.12] one can conclude that the dependence of $I_k(\epsilon, s)$, $k = 1, 2, 3$, on ϵ is due only to the limits of integration. By means of simple but tedious calculations we expanded each of the three integrals $I_1(\epsilon, s)$, $I_2(\epsilon, s)$, and $I_3(\epsilon, s)$ in series with respect to the powers of ϵ. The result read

$$I_1(\epsilon, s) = O(\epsilon^4) \quad [A.14]$$

$$2I_2(\epsilon, s) + I_3(\epsilon, s) = G_0(s) + \epsilon^2 G_1(s) + O(\epsilon^4), \quad [A.15]$$

where $G_0(s)$ and $G_1(s)$ are given by Eqs. [3.13] and [3.16]. Finally, substitution from [A.14] and [A.15] into [A.7], along with [A.3], yields Eq. [3.15].

ACKNOWLEDGMENTS

This study was supported by the Committee for Science and Higher Education of Bulgaria. The authors are indebted to Professor P. Bothorel, Dr. A. D. Nikolov, Dr. H. F. Eicke, Dr. A. M. Cazabat, and Dr. D. Langevin for stimulating discussions.

REFERENCES

1. Dore, J. C., Grimson, M. J., Langevin, D., and Robinson, B. H., *Rep. Prog. Phys.*, in press.
2. Widom, B., *J. Chem. Phys.* **81,** 1030 (1984).
3. Robledo, A., "Statistical Mechanical Models for Micellar Solutions and Microemulsions," Instituto de Fisica, Universidad Nacional Autonoma de Mexico, Mexico, 1987.
4. Brunetti, S., Roux, D., Bellocq, A. M., Fourche, G., and Bothorel, P., *J. Phys. Chem.* **87,** 1028 (1983).
5. Cazabat, A. M., and Langevin, D., *J. Chem. Phys.* **74,** 3148 (1981).
6. Calje, A. A., Agterof, W. G. M., and Vrij, A., *in* "Micellization, Solubilization, and Microemulsions" (K. L. Mittal, Ed.), Vol. 2, p. 779. Plenum, New York/London, 1977.
7. Cazabat, A. M., *in* "Physics of Amphiphiles: Micelles, Vesicles, and Microemulsions," p. 723. XC Corso, Bologna, 1985.
8. Ober, R., and Taupin, C., *J. Phys. Chem.* **84,** 2418 (1980).
9. Hou, M. J., Kim, M., and Shah, D. O., *J. Colloid Interface Sci.* **123,** 398 (1988).
10. Felderhof, B. U., *J. Phys. A: Math. Gen.* **11,** 929 (1978).
11. Guering, P., and Cazabat, A. M., *J. Phys. Lett.* **L44,** 601 (1983).
12. Chatenay, D., Urbach, W., Cazabat, A. M., and Langevin, D., *Phys. Rev. Lett.* **54,** 2253 (1985).
13. Scriven, L. E., *in* "Micellization, Solubilization, and Microemulsions" (K. L. Mittal, Ed.), Vol. 2, p. 877. Plenum, New York/London, 1977.
14. Auvray, L., *J. Phys. Lett.* **46,** 163 (1985).
15. Hill, T. L., "An Introduction to Statistical Thermodynamics." Addison–Wesley, Reading, MA, 1960.
16. Lagues, M., Ober, R., and Taupin, C., *J. Phys. Lett.* **39,** 487 (1987).
17. Zana, R., and Lang, J., *in* "Solution Behavior of Surfactants" (K. L. Mittal, Ed.), p. 1195. Plenum, New York, 1980.
18. Eicke, H. F., Shepherd, J. C., and Steineman, A., *J. Colloid Interface Sci.* **56,** 168 (1976).
19. Roux, D., Bellocq, A. M., and Bothorel, P., *in* "Surfactants in Solution" (K. L. Mittal and B. Lindeman, Eds.), Vol. 3, p. 1843. Plenum, New York, 1984.
20. Helfrich, W., *Z. Naturforsch. C Biosci.* **28,** 693 (1973).
21. de Gennes, P. G., and Taupin, C., *J. Phys. Chem.* **86,** 2294 (1982).
22. Mitchell, D. J., and Ninham, B. W., *J. Chem. Soc., Faraday Trans. 2* **77,** 601 (1981).
23. Ruckenstein, E., *J. Colloid Interface Sci.* **114,** 173 (1986).
24. Miller, C. A., *J. Dispersion Sci. Technol.* **6,** 159 (1985).
25. Robbins, M. L., *in* "Micellization, Solubilization, and Microemulsions" (K. L. Mittal, Ed.), Vol. 2, p. 713. Plenum, New York, 1977.
26. Safran, S. A., *J. Chem. Phys.* **78,** 2073 (1983).
27. Safran, S. A., *in* "Surfactants in Solution" (K. L. Mittal and B. Lindman, Eds.), V. 3, p. 1781. Plenum, New York, 1984.
28. Ivanov, I. B., and Dimitrov, D. S., *in* "Thin Liquid Films" (I. B. Ivanov, Ed.), p. 379. Dekker, New York, 1988.
29. Shah, D., Walker, R., Hshieh, W., Shah, N., Dwivedi, S., Nelander, J., Pepinski, R., and Deamer, D.,

SPE 5815, presented at Improved Oil Recovery Symposium of SPE of AIME, Tulsa, Oklahoma, 1976.

30. Bansal, V., Chinnaswamy, K., Ramachandran, C., and Shah, D., *J. Colloid Interface Sci.* **72,** 524 (1979).
31. Roux, D., Ph. D. Thesis, University of Bordeaux, 1984. [In French]
32. Chizmadzhev, Yu. A., and Pastushenko, V. F., *in* "Thin Liquid Films" (I. B. Ivanov, Ed.), p. 1059. Dekker, New York, 1988.
33. Maldarelli, C., and Jain, R. K., *in* "Thin Liquid Films" (I. B. Ivanov, Ed.), p. 379. Dekker, New York, 1988.
34. Maldarelli, C., Jain, R. K., Ivanov, I. B., and Ruckenstein, E., *J. Colloid Interface Sci.* **78,** 118 (1980).
35. Ivanov, I. B., Jain, R. K., Somasundaran, P., and Traikov, T. T., *in* "Solution Behavior of Surfactants" (K. L. Mittal, Ed.), Vol. 2, p. 817. Plenum, New York, 1979.
36. Eicke, H. F., *in* "Interfacial Phenomena in Apolar Media" (H. F. Eicke and G. D. Parfitt, Eds.), p. 41. Dekker, New York, 1988.
37. Chen, S. J., Evans, D. F., and Ninham, B. W., *J. Phys. Chem.* **88,** 1631 (1984).
38. Angel, L. R., Evans, D. F., and Ninham, B. W., *J. Phys. Chem.* **87,** 538 (1983).
39. Ono, S., and Kondo, S., "Molecular Theory of Surface Tension in Liquids," Handbuch der Physik, Vol. 10. Springer-Verlag, Berlin, 1960.
40. Rusanov, A., "Phasengleichgewichte und Grenzflachenerscheinungen" Academie-Verlag, Berlin, 1978.
41. Ivanov, I. B., and Kralchevsky, P. A., *in* "Thin Liquid Films" (I. B. Ivanov, Ed.), p. 49. Dekker, New York, 1988.
42. Gurkov, T. D., and Kralchevsky, P. A., *Colloids Surf.,* in press.
43. Hamaker, H. C., *Physica* **4,** 1058 (1937).
44. Nir, S., and Vassilieff, C. S., *in* "Thin Liquid Films" (I. B. Ivanov, Ed.), p. 207. Dekker, New York, 1988.
45. Evans, J. M., *in* "Light Scattering from Polymer Solutions" (M. B. Huglin, Ed.), p. 89. Academic Press, New York, 1972.
46. Visser, J., *Adv. Colloid Interface Sci.* **3,** 331 (1972).
47. Gracia, A., Thesis, Université de Pau (1978).
48. Biais, J., Barthe, M., Clin, B., and Lalanne, P., *J. Colloid Interface Sci.* **102,** 361 (1984).
49. Ter-Minassian-Saraga, L., *in* "Proceedings of the 31st International Congress of Pure and Applied Chemistry," Sofia, 1987.
50. Dichristina, T., Roux, D., Bellocq, A. M., and Bothorel, P., *J. Phys. Chem.* **89,** 1433 (1985).
51. Davies, J., and Rideal, E., "Interfacial Phenomena," p. 232. Academic Press, New York, 1963.
52. Fischer, E. W., *Kolloid Z.* **160,** 120 (1958).
53. Napper, D. H., "Polymeric Stabilization of Colloidal Dispersions," Academic Press, New York, 1983.
54. Hildebrand, E. A., McKinnon, I. R., and MacFarlane, D. R., *J. Phys. Chem.* **90,** 2784 (1986).
55. Rulyov, N. N., and Dukhin, S. S., *Kolloidn. Zh.* **48,** 302 (1986).